Sensitive Amperometric Immunosensing Using Polypyrrolepropylic Acid Films for Biomolecule Immobilization

ARTICLE *in* ANALYTICAL CHEMISTRY · DECEMBER 2006

Impact Factor: 5.64 · DOI: 10.1021/ac060657o · Source: PubMed

6 AUTHORS, INCLUDING:

Hua Dong
South China University of Technology
44 PUBLICATIONS **1,484** CITATIONS
SEE PROFILE

Chang Li
Xin Xiang Medical University
392 PUBLICATIONS **13,138** CITATIONS
SEE PROFILE

John H.T. Luong
321 PUBLICATIONS **10,176** CITATIONS
SEE PROFILE

Sensitive Amperometric Immunosensing Using Polypyrrolepropylic Acid Films for Biomolecule Immobilization

Hua Dong,[†] Chang Ming Li,[*,†] Wei Chen,[†] Qin Zhou,[†] Zhao Xian Zeng,[‡] and John H. T. Luong[†,§]

School of Chemical and Biomedical Engineering, Nanyang Technological University, Nanyang Avenue, Singapore 639798, Watson Pharma, Inc., 620 North 51st Avenue, Phoenix, Arizona 85043, and Biotechnology Research Institute, National Research Council Canada, Montreal, Quebec, Canada H4P 2R2

An electrochemical immunosensor was constructed using an electropolymerized pyrrolepropylic acid (PPA) film with high porosity and hydrophilicity. A high density of carboxyl groups of PPA was used to covalently attach protein probes, leading to significantly improved detection sensitivity compared with conventional entrapment methods. As a model, anti-mouse IgG was covalently immobilized or entrapped in the PPA film and used in a sandwich-type alkaline phosphatase-catalyzing amperometric immunoassay with *p*-aminophenyl phosphate as the substrate. With covalent binding, the detection limit for IgG in PBS buffer, pH 7.4, was 100 pg/mL with a dynamic range of 5 orders of magnitude. The covalent bonding mode in the carbonate−bicarbonate buffer, pH 9.6, further brought down the detection limit to 20 pg/mL with remarkable selectivity.

Immunosensing, a combination of specific immunoreaction with sensitive optical or electrochemical transduction, has attracted much attention since the 1970s.[1−4] Owing to the adaptability of electrochemical sensing to miniaturization, considerable research efforts have focused on electrochemical arrayed immunosensors and biochips with high sensitivity and specificity. One of the key steps in the construction of electrochemical immunosensors is to select a pertinent method for probe immobilization. The most widely used method is the bead-based immobilization technique where probes are physically adsorbed or covalently bound to the surface of polystyrene microbeads with a magnetic iron core.[5−6] Although high sensitivity (femtomoles) has been reported,[7] this approach cannot provide reproducible and addressable deposition of relevant immunoreagents with controlled spatial resolution, thus limiting its application in microarray and biochips. Another alternative method is to employ an electropolymerized conducting polymer as a matrix to immobilize immunoreagents. After the pioneering work of Foulds and Lowe,[8] the immobilization of biomolecules such as enzymes, DNA, antibodies, and even whole cells in conducting polymers has been widely studied to fabricate biosensors, including immunosensors. Compared with the bead-based method, the electrosynthesis of conducting polymers allows for precise control of probe immobilization on surfaces regardless of their size and geometry.[9] Since the polymerization occurs on the electrode surface, the probes are essentially entrapped in proximity to the electrode. This feature is of particular importance toward the development of sensing microelectrodes and microelectrode arrays to shorten the response time and alleviate interference from the bulk solution. Furthermore, the amount of immobilized probes can be easily controlled either by changing their concentration or by adjusting the thickness of the polymer matrix through the electrode potential, electropolymerization time, or both.

Among all of the conducting polymers studied up to date, polypyrrole (PPy) can be considered as one of the most attractive materials due to its excellent conductivity, stability, and biocompatibility even in neutral pH medium.[10,11] At present, most PPy-based immunosensors are performed with impedance or potential-step methods by measuring the changes in capacitance or resistance induced in antigen−antibody binding events, offering real-time and label-free measurement.[12−16] However, there are few

* To whom correspondence should be addressed. E-mail: ecmli@ntu.edu.sg.
† Nanyang Technological University.
‡ Watson Pharma, Inc.
§ Biotechnology Research Institute.

(1) Bauer, C. G.; Eremenko, A. V.; Ehrentreich-Forster, E.; Bier, F. F.; Makower, A.; Halsall, H. B.; Heineman, W. R.; Scheller, F. W. *Anal. Chem.* **1996**, *68*, 2453−2458.
(2) Honda, N.; Inaba, M.; Katagiri, T.; Shoji, S.; Sato, H.; Homma, T.; Osaka, T.; Saito, M.; Mizuno, J.; Wada, Y. *Biosen. Bioelectron.* **2005**, *20*, 2306−2309.
(3) Aguilar, Z. P.; Vandaveer, W. R.; Fritsch, I. *Anal. Chem.* **2002**, *74*, 3321−3329.
(4) Wang, J.; Tian, B.; Rogers, K. R. *Anal. Chem.* **1998**, *70*, 1682−1685.
(5) Kim, S. K.; Hesketh, P. J.; Li, C. M.; Thomas, J. H.; Halsall, H. B.; Heineman, W. R. *Biosen. Bioelectron.* **2004**, *20*, 887−894.
(6) Choi, J. W.; Oh, K. W.; Thomas, J. H., Heineman, W. R.; Halsall, H. B.; Nevin, J. H.; Helmicki, A. J.; Henderson, H. T.; Ahn, C. H. *Lab Chip* **2002**, *2*, 27−30.
(7) Bange, A.; Halsall, H. B.; Heineman, W. R. *Biosen. Bioelectron.* **2005**, *20*, 2488−2503.
(8) Foulds, N. C.; Lowe, C. R. *Anal. Chem.* **1988**, *60*, 2473−2478.
(9) Ionescu, R. E.; Gondran, C.; Gheber, L. A.; Marks, R. S. *Anal. Chem.* **2004**, *76*, 6808−6813.
(10) Ramanavicius, A.; Habermüller, K.; Csöregi, E.; Laurinavicius, V.; Schuhmann, W. *Anal. Chem.* **1999**, *71*, 3581−3586.
(11) Deore, B.; Chen, Z.; Nagaoka, T. *Anal. Chem.* **2000**, *72*, 3989−3994.
(12) Li, C. M.; Chen, W.; Yang, X.; Sun, C. Q.; Gao, C.; Zheng, Z. X.; Sawyer, J. *Frontier Biosci.* **2005**, *10*, 2518−2526.
(13) Gebbert, A.; Alvarez-Icaza, M.; Stocklein, W.; Schmid, R. D. *Anal. Chem.* **1992**, *64*, 997−1003.
(14) Sargent, A.; Loi, T.; Gal, S.; Sadik, O. A. *J. Electroanal. Chem.* **1999**, *470*, 144−156.
(15) Kalab, T.; Skladal, P. *Anal. Chim. Acta* **1995**, *4*, 361−368.

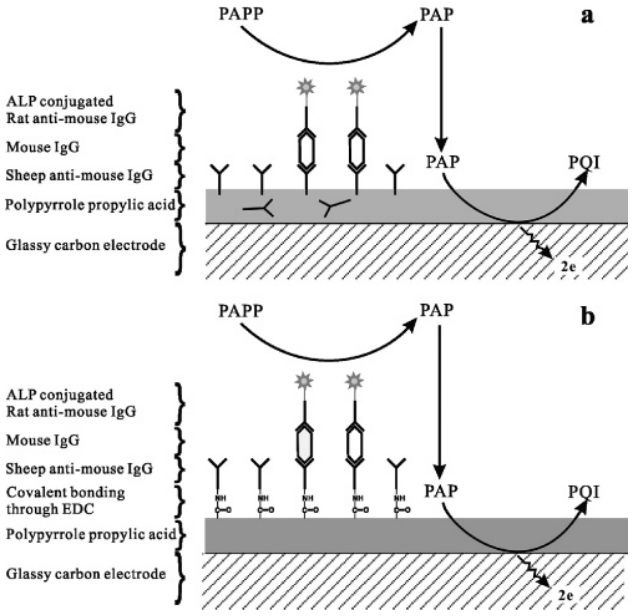

Figure 1. Schematic of the amperometric enzyme immunosensor based on the polypyrrolepropylic acid (PPA) film. The electroactive product, *p*-aminophenol (PAP), was converted from the enzymatic conversion of PAPP by alkaline phosphatase (ALP): (a) entrapment mode; (b) covalent bonding mode using EDC as the cross-linker.

reports on PPy-based amperometric immunosensors using a labeled enzyme to catalyze a substrate into a detectable electroactive product. The lack of widespread applications of PPy for amperometric immunosensing can be attributed to the poor permeability of PPy that hinders the diffusion of the electroactive product in and out of the polymer film.[9]

This paper describes the construction of a new amperometric immunosensor using electrosynthesized polypyrrolepropylic acid (PPA) as immobilization matrix. Probes can be attached to the abundant carboxyl groups on the polymer surface or entrapped in the polymer network, leading to fast and reliable amperometric responses. In our studies, mouse IgG is selected as a model analyte and its detection is realized in the presence of *p*-aminophenyl phosphate (PAPP) using the sandwich mode with rat anti-mouse IgG and sheep anti-mouse IgG (conjugated to alkaline phosphatase) as the primary and second antibodies, respectively (Figure 1). The performance of immunosensing with respect to detection sensitivity and reliability is presented and discussed in detail.

EXPERIMENTAL SECTION

Chemicals and Materials. Pyrrole was purchased from Aldrich (Madison, WI) and distilled prior to use. Glassy carbon electrodes (3 mm in diameter) were purchased from CH Instruments (Austin, TX). Alkaline phosphatase-conjugated Affinipure rat anti-mouse IgG (H+L), Chrompure mouse IgG, and biotin-SP conjugated Affinipure sheep anti-mouse IgG F(ab′)$_2$ were obtained from Jackson ImmunoResearch Laboratories (West Grove, PA). The cross-linker, 1-ethyl-3-(3-dimethylaminopropyl)carbodiimide hydrochloride (EDC) was purchased from Pierce (Rockford, IL).

(16) Ramanaviciene, A.; Ramanavicius, A. *Biosen. Bioelectron.* **2004**, *20*, 1076−1082.

Scheme 1. Chemical Synthesis of Pyrrolepropylic Acid (PPA)

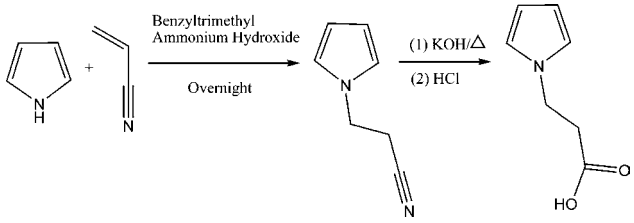

Human serum was purchased from Sigma (Madison, WI). The enzyme substrate, PAPP, was synthesized as described in the literature.[17] In brief, 1 mL of *p*-nitrophenyl phosphate (PNPP; Sigma, St. Louis, MO) and 10 mL of 0.05 M H_2SO_4 were added to the cathode chamber, separated in the electrolytic cell by a Nafion membrane (Aldrich), where Pt foils were used as the cathode and anode electrodes. Electrolysis was carried out using the galvanostatic mode at 8 mA/cm^2 for 5 h, and the resulting solution was adjusted to pH 9.0 with sodium hydroxide. The deionized water (18.2 MΩ·cm) was obtained from a Millipore Milli-Q water purification system. All other reagents were of analytical grade with highest purity.

Synthesis of Pyrrolepropylic Acid. Different methods to electrochemically synthesize polypyrrole have been extensively studied and reported.[18] PPA was prepared according to the following protocol: 3.8 mL of pyrrole (55 mmol) and 0.3 mL of benzyltrimethylammonium hydroxide were admixed, and then 2.9 mL of acrylonitrile (55 mmol) was added gradually to keep the temperature below 40 °C. After overnight stirring, the resulting mixture was hydrolyzed by adding 50 mL of potassium hydroxide (10 M) and refluxed overnight. The solution was cooled, and HCl was gradually added to acidify the solution to pH 3. The aqueous layer was extracted with ethyl acetate four times, each time with 30 mL of solvent. The combined organic layer was washed with 75 mL of brine and then dried with anhydrous magnesium sulfate. After solvent evaporation, the crude product was crystallized by methylene chloride and hexane. About 5 g of pure pyrrolepropylic acid was obtained (65% yield). ^{1}NMR ($CDCl_3$): 2.83 (t, 2H, J = 7.2 Hz), 4.20 (t, 2H, J = 7.2 Hz), 6.14 (t, 2H, J = 2.1 Hz), 6.67 (t, 2H, J = 7.2 Hz), 9.00 ppm (s, bd peak, 1H). The reaction can be summarized in (Scheme 1).

Electrochemical Instrumentation. Electropolymerization, cyclic voltammetry and differential pulse voltammetry were performed with an Autolab potentiostat/galvanostat (PGSTAT30, Eco Chemie B.V., Utrecht, The Netherlands). Before measurement, glassy carbon (GC) electrodes were polished with 0.3-μm γ-alumina powder, rinsed with deionized water, and then polished with 0.05-μm powder. After polishing, the electrodes were ultrasonically cleaned for 10 min in deionized water and finally soaked in acetone for 5 min, followed by vigorously washing with deionized water. Cyclic voltammograms of the polished electrodes were measured in 0.05M $Fe(CN)_6^{3-}/Fe(CN)_6^{4-}$ to confirm that the potential difference between cathodic and anodic peaks was not more than 65 mV (the theoretical value is ∼59 mV).

(17) Dong, H.; Li, C. M.; Zhou, Q.; Sun, J. B.; Miao, J. M. *Biosens. Bioelectron.* In press.

(18) Li, C. M.; Sun, C. Q.; Chen, W.; Pan, L. *Surf. Coat. Technol.* **2005**, *198*, 474−477.

Otherwise, the electrode was reconditioned until the desired result was obtained. All experiments were conducted using a three-electrode system, with a Pt wire and Ag/AgCl (saturated KCl) as counter and reference electrodes, respectively.

Electrochemical impedance spectroscopy (EIS) was used to characterize the PPA film formation, probe immobilization, and antigen−antibody interaction using an Autolab potentiostat/galvanostat (PGSTAT30) equipped with a frequency response analyzer module. All impedance data were recorded at an open circuit voltage with an amplitude of 10 mV over a frequency range of 1 Hz−1 MHz in 0.1 M PBS solution containing 10 mM $Fe(CN)_6^{3-}/Fe(CN)_6^{4-}$.

AFM Characterization. To substantiate the difference between the electrochemical behavior of PPy and PPA, the surface morphology of the PPy and PPA films, respectively was characterized by AFM (Nanoman, Veeco, Santa Barbara, CA) using tapping mode and operating in air.

FT-IR Characterization. To identify the main functional groups on the surface of electropolymerized PPA films, attenuated total reflection Fourier transform infrared (ATR-FT-IR) spectroscopy was performed by using the Nicolet Magna IR 560 ESP spectrophotometer (Thermo Nicolet, Madison, WI) incorporated with a "Golden Gate" ATR module (Graseby Specac, Smyrna, GA). The IR data show that the strongest peak appears at 1730 cm^{-1}, which can be assigned to C=O in carboxyl groups, suggesting the abundance of carboxyl groups in the PPA film.

Immunosensor Construction. Two methods were used for probe immobilization. For covalent bonding, PPA monomers were first electropolymerized on the GC electrode to form a PPA film by the galvanostatic method at 0.1 mA for 500 s. The coated electrode was washed three times with 0.1 M PBS and dried under a gentle nitrogen stream. The electrode was then immersed in 150 μL of acetonitrile (ACN) containing 1.5 wt % EDC for 1.5 h at room temperature. After careful rinsing with ACN, the electrode was exposed to a solution containing 100 μg/mL sheep anti-mouse IgG for 2 h, followed by washing and 1% BSA treatment for 2 h to alleviate nonspecific protein adsorption. The resulting electrode was incubated with different concentrations of mouse IgG (0.1 ng/mL to 1 μg/mL) for 2 h followed by washing with PBS. Thereafter, 100 μL of 20 μg/mL rat anti-mouse IgG (H+L) conjugated alkaline phosphatase (ALP) was dropped onto the electrode surface and incubated for 2 h. Finally, all the modified electrodes were rinsed with PBS before electrochemical measurement. In the entrapment method, 0.3 M PPA was mixed with 100 μg/mL sheep anti-mouse IgG and then electrochemically polymerized to form a protein-doped PPA film. Incubation of antigen and binding of the second antibody were similar to that described above.

Amperometric Measurement. The sandwich immunoassay was performed by dropping 150 μL of PAPP solution to cover the modified immunosensor. Differential pulse voltammetry (DPV) was used to detect amperometric responses because of its high signal-to-noise (S/N) ratio. In the DPV measurement, the pulse amplitude, pulse width, sampling width, and pulse period were 50 mV and 0.06, 0.02, and 0.2 s, respectively, and the potential range was −0.4 to +0.3 V versus Ag/AgCl.

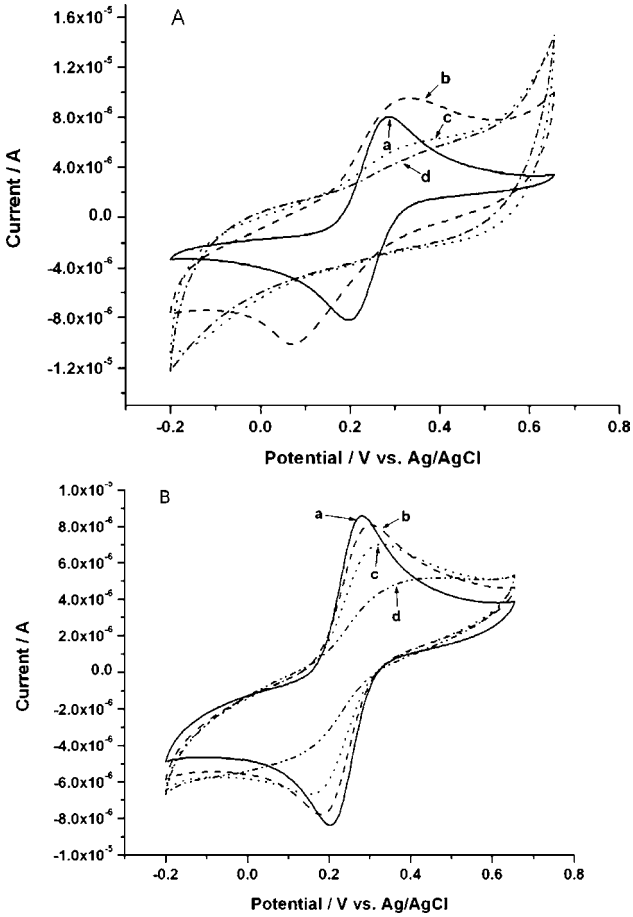

Figure 2. Cyclic voltammograms of 50 μM $Fe(CN)_6^{3-}/Fe(CN)_6^{4-}$ on polymer-coated GC electrodes with the scan range of −0.2 to +0.65 V vs Ag/AgCl. (A) PPy electropolymerized with the charge of 0 (a), 1 (b), 2 (c), and 3 mC (d). (B) PPA electropolymerized with the charge of 0 (a), 10 (b), 20 (c), and 30 mC (d). Scan rate, 50 mV/s.

RESULTS AND DISCUSSION

Electrochemical Behavior of the PPy and PPA Films. Figure 2 compares the cyclic voltammograms (−0.2 to +0.65 V vs Ag/AgCl) of $Fe(CN)_6^{3-}/Fe(CN)_6^{4-}$ obtained on the PPy- and PPA-coated GC electrodes in 0.1 M PBS at pH 7.4. The film thickness was controlled by the charge passing during the electropolymerization step. Replacement of HN in pyrrole by the propylic acid group (CH_2CH_2COOH) resulted in different electrochemical behavior. During the growth of the PPy film, the redox peak current of $Fe(CN)_6^{3-}/Fe(CN)_6^{4-}$ declined sharply whereas the peak potential separation between anodic and cathodic waves increased drastically. Indeed, the 3-mC-thick PPy film did not display defined redox waves for $Fe(CN)_6^{3-}/Fe(CN)_6^{4-}$, indicating both the deactivation of PPy and the poor permeability of $Fe(CN)_6^{3-}/Fe(CN)_6^{4-}$ through the polymer film. Since most of electroactive products such as H_2O_2 converted from the enzyme catalytic reaction exhibit higher positive oxidation potentials compared to the PPy film, the continual detection of these electroactive species will keep the polymer in an oxidized state for a long time and cause the loss of polymer conductivity, namely, deactivation.[19−25] Even the oxidation potential of electroactive

(19) Wang, J.; Musameh, M. *Anal. Chim. Acta* **2005**, *539*, 209−213.
(20) Gao, M.; Dai, L.; Wallace, G. G. *Synth. Met.* **2003**, *137*, 1393−1394.

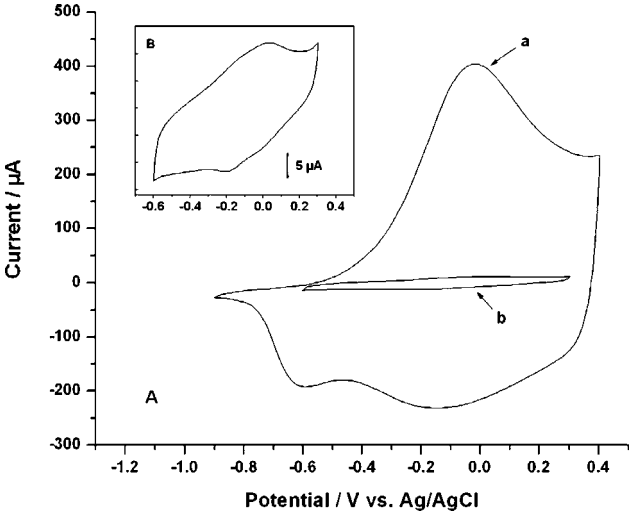

Figure 3. (A) Comparison of polymer conductivity between PPy (curve a) and PPA (curve b) in 0.1 M PBS solution (pH 7.4) using cyclic voltammetry; (B, inset) amplified CV curve of PPA. Scan rate, 50 mV/s.

products such as PAP is close to that of PPy; the electrooxidation of PPy (doping) in a broad potential range will increase the background current and thus decreases the S/N ratio. In addition, the dense structure and hydrophobic property of the PPy film after polymerization restrict the permeation of electroactive species to the electrode surface. Without reconditioning (overoxidation),[19] the signal response of the PPy-coated electrode is very weak and undetectable, particularly at low analyte concentrations.

In contrast, the redox waves of $Fe(CN)_6^{3-}/Fe(CN)_6^{4-}$ (curves a and b in Figure 2B) were almost identical even if the PPA film thickness increased from 0 to 10 mC. The peak current and potential separation were only slightly changed compared to the bare GC electrode (Figure 2B, curve a). For the 30-mC film thickness, the redox peaks (curve d in Figure 2B) were still observable but decreased gradually with the growth of the film thickness. This behavior was reasoned to result from the deactivation of PPA or the retarded diffusion of $Fe(CN)_6^{3-}/Fe(CN)_6^{4-}$ through the polymer film. To decipher this behavior, cyclic voltammograms of PPA and PPy measured in the PBS buffer were used to estimate their conductivity. A pair of redox peaks in the PPA polymer was observed at ~0.0 and −0.2 V versus Ag/AgCl (Figure 3, curve b), implying that the PPA film might also possess a doping and undoping process like PPy (Figure 3, curve a). However, the peak current of PPA was much lower compared with that of PPy, indicative of poor conductivity of the PPA film. Besides, it was found that the electropolymerization potential of PPA was ~2.3 V versus Ag/AgCl, compared to ~0.82 V for PPy under the same conditions. In other words, the deposition of PPA film required higher overpotential than the level required for the PPy film. On this basis, the PPA film could not be subjected to the loss of conductivity (or, namely, deactivation) even if held at high positive potential for a long period. Therefore, the decay in the redox peaks (Figure 2B) was mainly caused by the limited diffusion of $Fe(CN)_6^{3-}/Fe(CN)_6^{4-}$ into a thick PPA membrane.

The same experiment was also carried out with PAP, the enzyme-catalytic product of PAPP, as an indicator. Similarly, that is, the PPy film drastically hindered the permeation of PAP while the PPA film appeared much more permeable. The CV curves of PAP and $Fe(CN)_6^{3-}/Fe(CN)_6^{4-}$ recorded on PPA-coated electrodes both exhibited the increasing peak currents with the growth of cycles, which proved the mass-transfer process of PAP and $Fe(CN)_6^{3-}/Fe(CN)_6^{4-}$ diffusion through the polymer film. However, the time required for PAP to reach its maximum peak current was much shorter compared to that for $Fe(CN)_6^{3-}/Fe(CN)_6^{4-}$, indicating a faster diffusion rate of PAP. A rationale behind such behavior could be explained as the electrostatic repulsion between the PPA film (negative charge) and $Fe(CN)_6^{3-}/Fe(CN)_6^{4-}$. As a consequence, the permeation of $Fe(CN)_6^{3-}/Fe(CN)_6^{4-}$ was reduced. Obviously, the fast diffusion rate of PAP in the PPA film would lead to the reduced response time of the immonosensor.

Structural Characteristics of the PPA Film. Under positive potential and with long exposure, PPy gradually loses its conductivity due to the destruction of long-range conjugation in the polymer.[24] Thus, amperometric responses from electroactive species in the solution cannot be detected on the deactivated PPy surface. In the case of PPA with poor conductivity, the signal response was always observed regardless of the duration in which the polymer was kept at a positive potential. This result could only be explained by the difference in the polymer structures. In our experiment, AFM was used to probe the PPA film. The AFM micrographs of the bare GC electrode (Figure 4a,b) displayed some scrapping traces, caused by 0.05-μm alumina powder during electrode cleaning and polishing. When the electrode was covered with the polypyrrolepropylic acid film, the AFM micrograph illustrated a porous structure without any appearance of scrapping traces (Figure 4c,d). The aperture size was mainly distributed over 0.2−0.5 μm, which was sufficient for the permeation of ions. The formation of the porous structure was not totally unexpected since electrons could not efficiently transfer through the PPA film. Hence, a long-chain polymer could not be synthesized in the absence of free radicals, indicating a self-limiting process. From Figure 4c,d, the PPA film thickness was estimated to be ~100 nm after charging with 0.1 mA for 500 s. For comparison, the AFM images of the PPy film prepared under the same condition was measured (Figure 4e,f). Obviously, the structure of PPy was very compact without any observable pore on the polymer surface. As a result, ions such as $Fe(CN)_6^{3-}/Fe(CN)_6^{4-}$ and PAP cannot penetrate this film. Nevertheless, PPy could also become porous after overoxidation at a very high positive potential, resulting in detectable signals.[26,27] However, the activity of the immobilized biomolecules might be affected at high anodic potential when a single electropolarization step was used to entrap such biomolecules.

Characterization of Polymer Coating and Protein Immobilization/Binding Events on the Electrode Surface. Abun-

(21) Gros, P.; Comtat, M. *Biosen. Bioelectron.* **2004**, *20*, 204−210.
(22) Zeng, K.; Tachikawa, H.; Zhu, Z.; Davidson, V. *Anal. Chem.* **2000**, *72*, 2211−2215.
(23) Dai, Y. Q.; Shiu, K. K. *Electroanalysis* **2004**, *16*, 1697−1703.
(24) Ramanavicius, A.; Habermüller, K.; Csöregi, E.; Laurinavicius, V.; Schuhmann, W. *Anal. Chem.* **1999**, *71*, 3581−3586.
(25) Rangamani, A. G.; McTigue, P. T.; Verity, B. *Synth. Met.* **1995**, *68*, 183−190.
(26) Bélanger, D.; Nadreau, J.; Fortier, G. *J. Electroanal. Chem.* **1989**, *274*, 143−155.
(27) Cosnier, S. *Biosen. Bioelectron.* **1999**, *14*, 443−456.

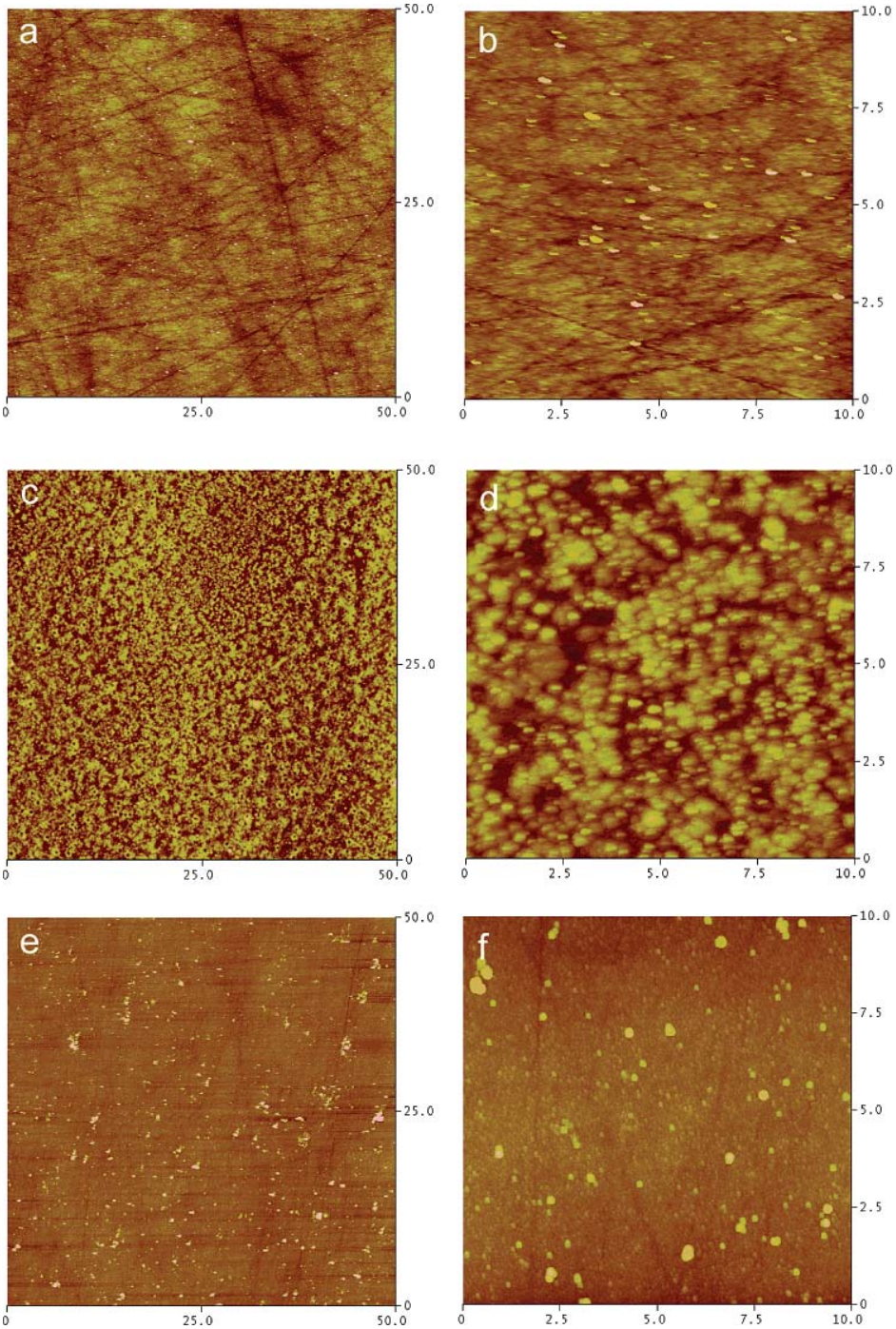

Figure 4. AFM images of the bare and coated GC electrodes. (a) and (b) Bare electrode surface after polishing with 0.05-μm alumina powder. Scan sizes are 50 and 10 μm. (c) and (d) PPA-coated electrode surface with the charge of 50 mC. (e) and (f) PPy-coated electrode surface with the charge of 50 mC.

dant carboxyl groups on the PPA polymer surface enhance the film hydrophilicity and enable probe immobilization via covalent bonding. To attest the attachment of antigen and antibody onto the electrode surface, EIS was used for monitoring the dynamics of the polymer and Ag−Ab interaction.[28] Due to the absence of an internal redox couple during the polymerization and protein immobilization/binding events, $Fe(CN)_6^{3-}/Fe(CN)_6^{4-}$ was added in the solution as the indicator to acquire faradic impedance spectra. Note that the attachment of polymer and proteins to the electrode surface retards the interfacial electron transfer of $Fe(CN)_6^{3-}/Fe(CN)_6^{4-}$ and thus increases the electron-transfer resistance.[29] Figure 5 illustrates the EIS profile, in which the Nyquist plot is shown with the real part (Z'') on the X-axis and the imaginary part (Z') on the Y-axis. The impedance spectra (a−e) in Figure 5 were measured on a GC electrode before and after the polymer coating, anti-mouse IgG immobilization, anti-mouse

(28) Sadik, O. A.; Xu, H. *Anal. Chem.* **2002**, *74*, 3142−3150.

(29) Ruan, C. M.; Yang, L. J.; Li, Y. B. *Anal. Chem.* **2002**, *74*, 4814−4820.

IgG/mouse IgG interactions, and the attachment of ALP conjugated rat anti-mouse IgG, respectively. The spectra illustrated well-defined semicircles at high frequencies followed by straight lines at low frequencies. The semicircle portion corresponded to the electron-transfer-limited process with its diameter equal to the electron-transfer resistance (R_{ct}). The straight line was formed by the diffusion control of the reactant species. The lowest electron-transfer resistance on the bare electrode (Figure 5a) indicated the fastest electron-transfer rate between the bare electrode and the $Fe(CN)_6^{3-}/Fe(CN)_6^{4-}$ pair. With the PPA film-coated surface (Figure 5b), the electron-transfer resistance increased dramatically, owing to the high electrode coverage by the PPA layer with poor conductivity. After probe antibody immobilization, antigen−antibody binding, and the second antibody attachment (Figure 5e), Faraday resistances R_{ct} increased accordingly, indicating the successful construction of the immunosensor. However, the increase in R_{ct} was not as drastic as that caused by the PPA film since the electrode surface was only subjected to low coverage of proteins. Such results confirmed the applicability of PPA in electrochemical impedance immunosensing.

Performance of the Immunosensor. Mouse IgG was used as the target protein in electrochemical sandwich immunoassay experiments, involving immobilization of the primary antibody (Ab, sheep anti-mouse IgG), capture of the analyte (Ag, mouse IgG), association of alkaline phosphatase conjugated rat anti-mouse IgG, and finally incubation in a PAPP solution.[3,30−32] For the detection, ALP converted PAPP to *p*-aminophenol (PAP), which was electrooxidized to *p*-quinone imine at ~0 V versus Ag/AgCl (eqs 1 and 2).

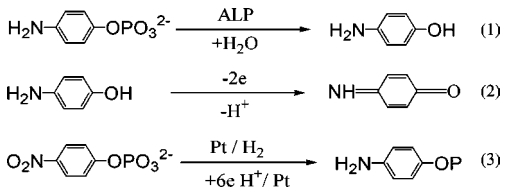

In our study, the enzyme substrate, PAPP was synthesized as described previously (Experimental Section). In brief, the nitro group in PNPP was electroreduced or chemically reduced by the hydrogen produced during electrolysis to form an amino group (eq 3).[17]

Differential pulse voltammetry (DPV) can be used to achieve sensitive responses from the immunosensor.[33] Figure 6 shows the differential pulse voltammograms of PAP measured with an interval time of 130 s. The concentration of target protein, mouse IgG, was 100 ng/mL, and the probe was covalently immobilized to the PPA film with EDC as the cross-linker. As shown in Figure 6, virtually no peak current was detected right after the addition of PAPP. With prolonged time, the peak current increased,

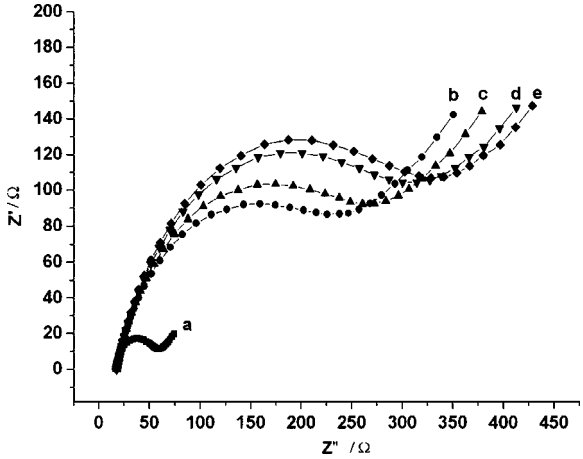

Figure 5. EIS of the PPA-coated GC electrode in 0.1 M PBS solution containing 10 mM $Fe(CN)_6^{4-}/Fe(CN)_6^{3-}$. (a) Bare electrode; (b) PPA-coated electrode; (c) modified with sheep anti-mouse IgG; (d) combined with mouse IgG; (e) coated with sandwich complexes of ALP-conjugated rat anti-mouse IgG.

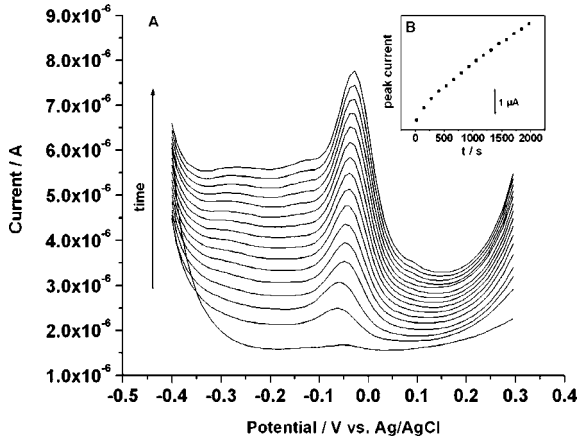

Figure 6. (A) DPV curves of PAP at various times with the increasing rate of 130 s by use of the covalent bonding mode; (B, inset) peak current dependence on time.

reflecting the increase in the PAP concentration. The peak current−time linear relationship (Figure 6B) indicated zero-order kinetics for the enzymatic reaction. The rate increase of the PAP concentration (the slope of I vs t) was proportional to the amount of enzyme conjugated to the second antibody, i.e., proportional to the amount of antigen to be detected. According to the DPV theory, the slope of I versus t is a function of the electrode surface area and the amount of enzyme. To normalize the surface area, all electrodes involved in the experiment were measured in the same PAP solution and their relative areas were obtained by comparing the obtained peak currents.

Figure 7A shows the calibration plot obtained with the covalent bonding mode; i.e., probes were covalently attached to the PPA surface. Measurements were performed in triplicate using three different immunosensors. A linear relationship was observed over the range of 100 pg/mL−1 μg/mL, illustrating the successful development of the PPA-based amperometric immunosensor. Besides covalent bonding, PPA could also serve as a matrix to directly entrap probes, thus simplifying the preparation of the immunosensors. The porous structure of the PPA film enables the target proteins to interact with the probes encapsulated in

(30) Ding, Y.; Zhou, L. P.; Halsall, H. B.; Heineman, W. R. *J. Pharm. Biomed.* **1999**, *19*, 153−161.
(31) Thomas, J. H.; Kim, S. K.; Hesketh, P. J.; Halsall, H. B.; Heineman, W. R. *Anal. Chem.* **2004**, *328*, 113−122.
(32) Honda, N.; Inaba, M.; Katagiri, T.; Shoji, S.; Sato, H.; Homma, T.; Osaka, T.; Saito, M.; Mizuno, J.; Wada, Y. *Biosen. Bioelectron.* **2005**, *20*, 2306−2309.
(33) Zhan, D. P.; Mao, S. N.; Zhao, Q.; Chen, Z.; Hu, H.; Jing, P.; Zhang, M. Q.; Zhu, Z. W.; Shao, Y. H. *Anal. Chem.* **2004**, *76*, 4128−4136.

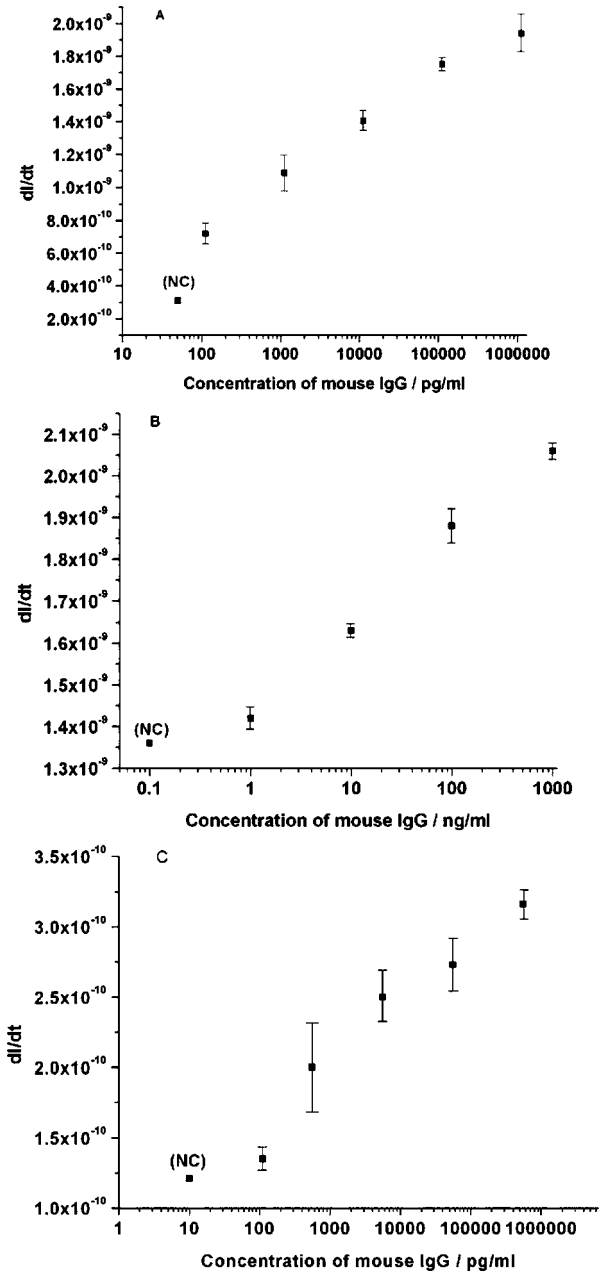

Figure 7. Calibration curves of mouse IgG using covalent bonding mode in PBS buffer (A), entrapment mode in PBS buffer (B), and covalent bonding mode in human serum (C). Detection at each concentration was repeated three times, and the results were averaged.

the polymer matrix. Figure 7B presents the corresponding calibration data, illustrating that the detection limit of the entrapment mode was an order higher than that of the covalent bonding mode. This could be ascribed to the higher concentration of probes immobilized in the PPA film by the covalent bonding method compared with the entrapment procedure.

The measurements were conducted in human serum at room temperature. Immunoglobulins (Ig) have five different Ig classes (IgG, IgM, IgD, IgA, IgE) based on differences in the constant region of the heavy chain. Frequent doses of antigen produced by infectious diseases usually lead to a strong IgG response in human serum. Thus, the immunosensor was validated in human

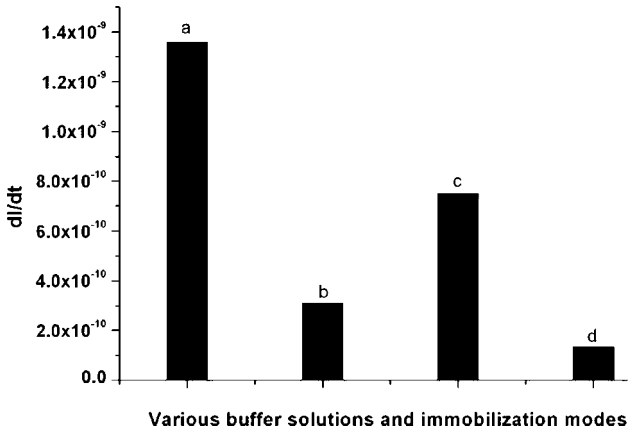

Figure 8. Amperometric responses at negative control in various buffer solutions. (a) Entrapment mode in PBS, pH 7.4; (b) covalent bonding mode in PBS; (c) entrapment mode in carbonate−bicarbonate, pH 9.6; (d) covalent bonding mode in carbonate−bicarbonate, pH 9.6.

serum for its specificity and sensitivity. The detection limit was observed in the same order range compared with the data obtained in PBS (Figure 7C), validating the high specificity of the proposed immunosensor.

To investigate the stability of immunosensors, the electrode was stored in PBS buffer at 4 °C and examined every 24 h, repetitively. The amperometric responses retained ~85% of the initial activity after 24 h and ~71% after 4 days. The results showed that the proposed immunosensor possesses satisfactory stability although biosensors are often designed as disposable devices in clinical practices.

Further Optimization of the Immunosensor. A series of experiments was performed to investigate the pH effect on the signal response and nonspecific interaction. The experimental results indicated that the background current decreased with an increase of the solution pH. Figure 8 compares the amperometric signals of the negative control in PBS, pH 7.4, and the carbonate−bicarbonate buffer, pH 9.6. In brief, the background current in the carbonate−bicarbonate buffer was suppressed significantly, showing reduced nonspecific adsorption of ALP on the PPA film in a solution at high pH. One of the possible reasons could be ascribed to the stronger electrostatic interaction between ALP and the PPA film at lower pH, resulting in a higher background. In PBS, pH 7.4, ALP acquires a positive charge (pI 8.17) while PPA carries a negative charge due to the presence of carboxylate anions. Thus, the amount of ALP nonspecifically adsorbed on the PPA-coated electrode surface at the negative control was not negligible even after the blocker treatment. However, above pH 8.17, ALP carries a negative charge. Apparently, this could significantly reduce the nonspecific binding of ALP on the PPA film caused by the electrostatic interaction. As a result of the optimization, ~20 pg/mL mouse IgG could be detected using the covalent bonding mode in the carbonate−bicarbonate buffer, which was 5 times lower than the detecting limit in PBS. It should be noted that the background current of the covalent bonding mode (Figure 8b,d) were much smaller than that of the entrapment bonding mode (Figure 8a,c). Such results could be attributed to the lower amount of nonspecific bound ALP on the PPA film by the covalent bonding mode.

In brief, the novelty of the immunosensor described herein consists of the porous structure and hydrophilic property of the PPA film, which enable the detection of amperometric responses from the electroactive product during the course of the immunoassay. The abundance of carboxyl groups on the polymer surface permits immunoreagent immobilization via covalent bonding, leading to high detection sensitivity compared with the traditional entrapment method. Following investigation on the use of polypyrrolepropylic acid together with electrochemical sensing, significant improvements with regard to sensitivity can be achieved. With high reproducibility, the technique could have great potential toward the development of miniaturized protein biochips for clinical, forensics, environmental, and pharmaceutical applications.

ACKNOWLEDGMENT

This work was financially supported by Nanyang Technological University, Singapore, under the Research Program for Bionanosystems and Electronic Biochips.

Received for review April 7, 2006. Accepted August 21, 2006.

AC060657O